# A High power, medium voltage, series-resonant converter for DC wind turbines

Dincan, Catalin Gabriel; Kjær, Philip Carne; Chen, Yu-Hsing; Munk-Nielsen, Stig; Bak, Claus Leth

*Published in:*
I E E E Transactions on Power Electronics

*DOI (link to publication from Publisher):*
10.1109/TPEL.2017.2770220

*Publication date:*
2018

*Document Version*
Accepted author manuscript, peer reviewed version

# High power, medium voltage, series resonant converter for DC wind turbines

Catalin Dincan, *Student Member, IEEE,* Philip Kjaer, *Senior Member, IEEE,* Yu-hsing Chen, Stig Munk-Nielsen, Claus Leth Bak, *Senior Member, IEEE,*

***Abstract*—A new modulation scheme is introduced for a single-phase series-resonant converter, which permits continuous regulation of power from nominal level to zero, in presence of variable input and output dc voltage levels. Rearranging the circuit to locate the resonant LC tank on the rectifier side of the high turns-ratio transformer combined with frequency control and phase-shifted inverter modulation keep transformer flux constant from nominal frequency down to DC, always in sub-resonant continuous or discontinuous conduction mode. This overcomes the principal deficit of series-resonant converters, and the resulting compact and efficient transformer, and soft-commutated inverter, present particular advantages in high-power, high-voltage applications, like DC offshore wind turbines. With transformer excitation frequency in hundreds of Hz range, line-frequency diodes can be employed in the high-voltage rectifier valve. Circuit operation and conduction modes, governing equations and sample waveforms are presented, together with experiments from a scaled demonstrator.**

***Index Terms*—resonant converter, phase-shifted modulation, medium voltage DC, medium frequency transformer, offshore wind farm, high voltage converter**

## NOMENCLATURE

| | |
|---|---|
| $C_r$ | Resonant (tank) capacitor. |
| $\delta$ | Inverter legs phase displacement. |
| $F_{sw}$ | Switching frequency. |
| $F_r$ | Resonant frequency. |
| $i_m$ | Transformer magnetizing current. |
| $i_{out}$ | Output current of the converter. |
| $i_{rp}$ | Primary resonant current. |
| $i_{rs}$ | Secondary resonant current. |
| $i_r$ | Rectified current |
| $L_r$ | Resonant (tank) inductor. |
| $L_m$ | Transformer magnetizing inductance. |
| $SRC$ | Series resonant converter. |
| $V_g$ | Inverter output voltage. |
| $V_g'$ | Inverter reflected voltage on secondary. |
| $V_o$ | Rectifier voltage. |
| $V_o'$ | Rectifier voltage reflected on primary. |
| $V_{Cr}$ | Resonant capacitor voltage. |
| $V_t$ | Resonant tank voltag |
| $\Delta V$ | Voltage difference between $V_g'$ and $V_o$. |
| $T_{sw}$ | Switching period. |
| $T_r$ | Resonant current pulse period. |
| $Z_c$ | Resonant tank characteristic impedance |

## I. INTRODUCTION

All authors are with the Department of Energy Technology, Aalborg University , Aalborg,Denmark. Email:cgd@et.aau.dk

PRESENT offshore wind farms use mainly HVAC cables to transmit the energy collected from wind turbines to onshore, while other solutions use HVAC up to a large rectifier and then to the mainland through HVDC cable lines. According to [1], [5] and [14], HVDC-connected wind farms could operate with higher efficiency when connected to a MVDC (Medium Voltage Direct Current) collection grid. A single line diagram for the wind farm with DC collector grid is shown in Fig. 1. The motivation stems from the prospect of reducing LCoE (levelized cost of energy) by as much as 3%, by improving the efficiency with 2% and reducing the bill of material (BoM) costs by at least 1% [1]. In the long term, it is expected that MVDC will compete with MVAC for green field distribution networks.

The introduction of DC technology for wind turbines has attracted a lot of interest in both academia and industry, as it promises many features, compared to classic AC solutions. First of all, the traditional low frequency transformers will be replaced with dc/dc converters that incorporate medium frequency transformers, while DC cables will replace AC cables. Considerable lower size and weight can be achieved on the magnetic components and cables losses are decreased. Second, DC turbines seem to be the preffered candidate for offshore wind farms located at distances higher then 100 km, mainly due to higher and more constant wind speed. The desired, but challenging component of such a DC turbine would be the MV dc/dc converter, which has to be designed for challenging requirements.

Following paragraphs will discuss important properties for such converters, give a short review of proposed topologies and finally present the proposed dc/dc topology for this application.

### A. Important dc/dc converter properties in DC turbine

Various DC turbine concept proposals exist. In [2] a medium frequency generator is interfaced to MVDC grid through a simple diode rectifier, while in [3], a non-isolated MMC topology is discussed. Considering the cost of developing a new offshore wind turbine, a solution for DC-connection should preferably maximize the re-use of design from existing AC-connected turbines. Hence, the starting point for our work is to maintain the generator and its rectifier which controls generator power (see Fig. 1), and only change the electrical circuit from the LV DC bus to the terminals of the turbine, while keeping the same functionalities. In todays AC-connected turbines, the DC/AC inverter controls the LV DC bus voltage by adjusting the output active power and the

This article has been accepted for publication in a future issue of this journal, but has not been fully edited. Content may change prior to final publication. Citation information: DOI 10.1109/TPEL.2017.2770220, IEEE Transactions on Power Electronics



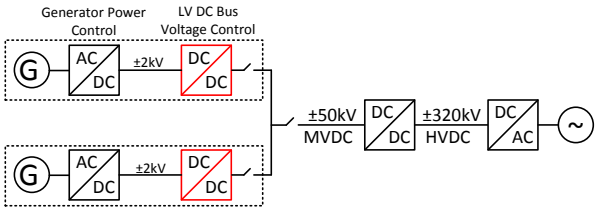


Fig. 1. Single line diagram of DC wind farm

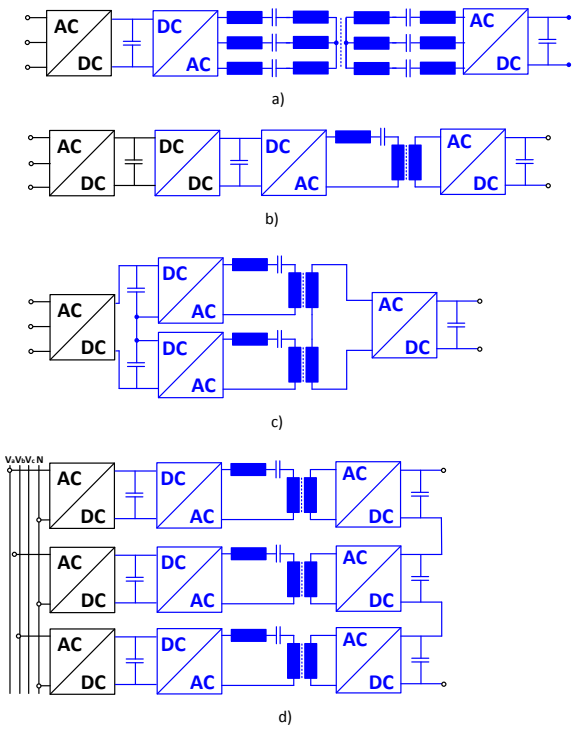


Fig. 2. Prior art in topology arrangements specific to SRCs: Booster controlled SRC (a); 3 phase SRC (b); Modular Multilevel SRC (c); per-phase approach of SRC (d).

transformer steps the voltage up. In a DC-connected turbine, the DC/DC converter will contain voltage transformation and control output power, too. To synthesize, the DC/DC converter should have following properties:

1) Ability to control LV DC bus voltage;
2) LVDC to MVDC voltage transformation ;
3) High efficiency across operational range;
4) Robust and compact design.

### B. Wind turbines dc/dc converters

Significant research has investigated various dc/dc converter topologies for DC turbines. Selecting an optimal topology is not straightforward, as all the proposed solutions are at an immature technology level both at system and component level, and no substantial experience from full scale detailed design exists.

Candidate circuits can be catalogued into hard-switching vs. soft-switching and non-isolated vs. isolated topologies. The advocates of non-isolated topologies claim that the design and manufacturing of high-frequency transformers with large turns ratio is difficult, mainly due to core materials costs, complicated cooling and high impact of stray parameters (such as stray capacitance and leakage inductance). Other problems include poor coupling, dielectric losses in insulation, core and windings losses from nonsinusoidal excitation, while the distributed capacitance of the winding turns can lower efficiency and prolonge the pulse transition [11]. A number of works has been proposed: [12] and [13] suggest a single and three phase topology, for both uni and bidirectional applications. They employ low-cost thyristors and use variable frequency for control. The topology is similar to a parallel resonant topology, but the high voltage stress across the semiconductors and resonant tank make it unsuitable for this application. In the same category, switched capacitor topologies where proposed in [14] and [15], each topology showing soft-switching capability, but require a large number of semiconductors and passive components.

In DC turbine application galvanic isolation is preferred, as it will offer increased personal safety and protection. The impact of stray parameters should be indeed considered if switching frequencies are in the range of tens or hundreds of kilohertz, which are specifications for high frequency pulse transformers. With MW- and kV-ratings, the transformer excitation is of hundreds of Hz, which may reduce impact of winding parasitic capacitance.

In one of the first works which have studied DC wind farms [5], the hard-switched full bridge converter was selected as preferred topology, but omitted the study of rectifier voltage overshoot and oscillations caused by transformer parasitic LC circuitry. [6] attempts a hard-switching 3-level NPC connected to the medium-frequency transformer via a passive filter, but efficiency is punished by hard-switching.

Further on, isolated soft-switching topologies like the single active bridge have been proposed in [1], [8] and [9] and offer a limited range of soft-switching capability, but suffer also from high voltage overshoots and oscillations, related to the high turns ratio of transformers.

### C. Review of SRC application in wind turbines

High availability, efficiency and power density should be design targets for the dc/dc converter and they can be achieved through the employment of high power resonant converters, as transformer non-idealities and stray parameters can be incorporated in the resonant tank, making them well-suited for high-voltage applications [24], [25].

The inspiration comes from traction and solid-state transformer (SST) applications, where demonstrators have been evaluated. Here, the classic series resonant converter (SRC) has been investigated in [16]-[20] for traction and in [21]-[23], for SSTs. Operated at constant frequency and in sub-resonant mode, the topology is known as the half cycle discontinuous-conduction-mode series-resonant converter (HC-DCM-SRC). For these particular applications, the converter basically cou-

This article has been accepted for publication in a future issue of this journal, but has not been fully edited. Content may change prior to final publication. Citation information: DOI 10.1109/TPEL.2017.2770220, IEEE Transactions on Power Electronics



ples two DC link voltages with a fixed voltage transfer ratio, but has no control possibilities.

For wind turbine application, interesting work was done in [10], where a three phase topology was introduced and further compared in [1] to the single and dual active bridge, promising efficiency above 99%, but without a means of controlling dc-link voltage (Fig. 2(a)).

There have been attempts of introducing resonant topologies that could offer control possibility, at this power and voltage level. A candidate solution (Fig. 2(b)) was proposed in [26] and it employs a SRC, operated at resonant mode and with constant frequency, while a front end boost converter controls the input DC-link, increasing the number of components, complexity and losses. In [31] a resonant topology consisting of multiple strings of switch pairs and multiple modules of resonant circuits (Fig. 2(c)) is proposed. [32] has also suggested a per phase approach (Fig. 2(d)), based on series resonant converter, while being operated at constant frequency and variable duty cycle. On the other hand, it's not obvious how high efficiency could be obtained with that particular mode of operation as no efficiency study was given.

To achieve high effiency with possibility of LV DC bus voltage control, this paper proposes the unidirectional series resonant converter. The topology was developed from the classic series resonant converter (SRC, Fig. 3(a)) with tank on inverter side, where if operated with variable frequency control in sub-resonant mode (as seen in Fig. 3(c)), averaged output power becomes a function of number of current pulses sent to the load (Fig. 3(e) and (f)). With an ideal transformer or very large magnetizing inductance, where magnetizing current is neglected, inverter and rectifier semiconductor will experience ZVS at turn-on and ZCS at turn-off. But, for variable frequency below resonant point of LC tank, the core magnetic flux $\Phi$ will vary with the applied volt-seconds, as seen in Fig. 3(c), implying two aspects: transformer has to be designed for lowest frequency, leading to a bulky and heavy component and saturation will occur below design point. To overcome this, our work proposes a method of operation for the SRC, where variable frequency and phase shift control in sub-resonant conduction mode are applied (as seen Fig. 3(d)) and it is successful only if the resonant tank is placed on rectifier side side, as seen in Fig. 2(b). The topology will be referred as SRC# (Fig. 4), with the ratings from Table I and with a patent application [27] under progress. The suggested topology has following features:

1) Unidirectional power flow;
2) Provides galvanic isolation;
3) Provides functionality of controlling input LV DC bus voltage;
4) Maintains state of the art PMSG and its active rectifier;
5) Constant and very high efficiency across entire operational range due to soft-commutation of inverter and rectifier devices (ZVS at turn-on and low turn-off current for IGBTs, ZVS at turn-on and ZCS at turn-off for rectifier diodes)
6) Low size and weight due to the medium frequency transformer immersed in oil;

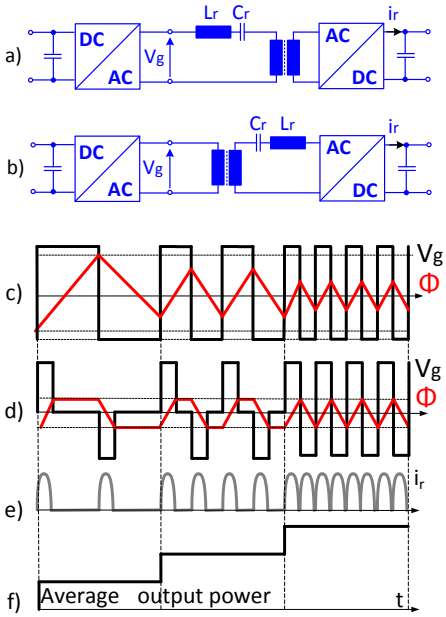


Fig. 3. SRC with tank on inverter side (a); SRC with tank on rectifier side (b); Inverter output voltage $V_g$ and magnetizing flux $\Phi$, for SRC with LC tank on inverter side and frequency controlled (c); Inverter output voltage $V_g$ and magnetizing flux $\Phi$, for SRC with LC tank on rectifier side and with pulse removal technique (d); Rectified current $i_r$ (e); Averaged output power, delivered to MVDC network (f).

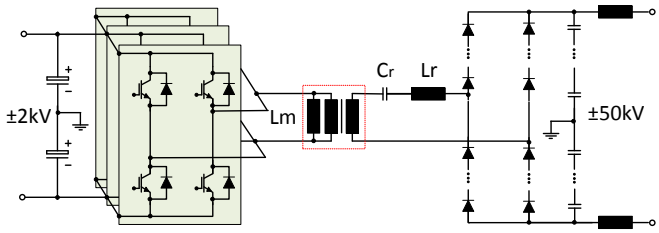


Fig. 4. Series resonant converter with new method of operation (SRC#);

7) Rectifier based on inexpensive line-frequency diodes, due to soft commutation and modest conversion frequency.

TABLE I
RATINGS FOR SRC#

| Parameter | Value |
|---|---|
| Nominal power, $P_n$ | 10 MW |
| Nominal input voltage, $V_{in}$ | ± 2kV |
| Nominal output voltage, $V_{out}$ | ± 50kV |
| Isolation level | ± 75 kV |
| Inverter | 4x3 in parallel IGBT(6500V-x-750A) |
| Rectifier | 4x40 in series diode (6500V-x-750A) |
| Frequency range $F_{sw}$ | 0-1000 Hz |
| Resonant capacitor $C_r$ | 0.250 uF |
| Resonant inductor $L_r$ | 78 mH |
| Transformer turns ratio, $N$ | 1:25 |
| Magnetizing inductance $L_m$ | 10 mH |

The paper is organized as follows: in Section II, operation principle of the SRC# is introduced, while its corresponding

conduction modes are described in section III. In Section IV, simulation results of steady state operation with the target converter are shown. Section V provides experiment results from a 1 kW prototype, confirming SRC# expected behaviour and Section VI concludes on the results.

## II. Operation principle of the SRC#

The series resonant converter with the new method of operation (SRC#) is depicted in Fig. 5(a) and comprises (from left to right) a full bridge inverter, one monolithic 1:N transformer, resonant LC tank and medium voltage rectifier. Power flows from $V_{in}$ to $V_{out}$. The switch pairs (S1/S2) and (S3/S4) as indicated in Fig. 6(e), operate at a 50% duty cycle. Commutation of switches on the leading leg (S1/S2) is phase shifted with respect to the conduction of switches on the lagging leg (S3/S4), with a duration $\delta$, equal to half of LC tank resonant period, resulting in a quasi-square excitation voltage as seen in Fig. 6(a). The applied square wave voltage passes through the transformer and excites the tank and a resonant tank current $i_{rs}$ starts to flow. After rectification and filtering it is fed into the medium voltage network, $V_{out}$. Up to this point there is no operational difference compared to a constant frequency phase shift control, which is normally applied for operation in super resonant mode, to achieve ZVS at turn on.

Considering the high power and medium voltage application in this case, 6.5 kV IGBTs will be employed on the inverter side, while 6.5kV line frequency diodes are used on rectifier side. As the main contributor to the overall losses with IGTB applications are the turn-off losses, sub-resonant mode is preferred as it allows ZCS or a small current at turn-off (see Fig. 5(b) and regardless of switching frequency, during every switching period a full resonant pulse is sent to the load. This mode facilites ZVS at turn-on and ZCS at turn-off for the rectifier diodes, as seen in Fig. 5(c). Further on, if frequency control is implemented, output power is dependent on the amount of energy transfer to the output stage, making it a function of number of energy pulses transferred to the output. Low frequency operation means low power output, while high frequency operation will deliver a high power output. On the other hand, the disadvantage of operating the SRC with resonant tank on inverter side in sub-resonant mode and frequency control, is that the transformer needs to be designed for the lowest frequency point and the magnetizing inductance needs therefore to be considered.

The question is now, how can the transformer be operated with variable frequency and be designed at highest operating frequency, while avoiding saturation at lower frequency. One possible way and with reference to Fig. 6(a), is to make $V_g$ a function of square wave pulses, meaning a pulse with determined length is applied to the inverter, but the distance between pulses varies as a function of output power. As the length of every voltage pulse is fixed, the amplitude of magnetizing current $i_m$ will be constant, as seen in Fig. 6(d). Further on and with ref. to Fig. 6(b), if the applied voltage $V_g$ has the same length as the resonant pulse $i_{rs}$, then frequency control in sub-resonant mode becomes possible, allowing the design of the transformer for highest operating point. This implies that LC tank resonant frequency $F_r$ will be equal or slightly higher then the maximum switching frequency $F_{sw}$, otherwise operation in sub-resonant mode is not possible. Power to frequency function is described in eq. (1):

$$P_{out} = 4 \cdot F_{sw} \cdot N \cdot C_r \cdot V_{in} \cdot V_{out} \quad (1)$$

## III. SRC# conduction modes

Considering that SRC# is operating in sub resonant mode, four modes of conduction (two discontinuous and two continuous) will appear under steady state operation: DCM1, DCM2, CCM1-hybrid and CCM1. Switching frequency $F_{sw}$ and voltage difference $\Delta V$ between primary reflected voltage $V_g$' (where $V_g$' = $V_g \cdot N$) and $V_o$ will determine whether the converter operates in one conduction state or another. Discontinuous modes are characterized by the number of half resonant cycles that appear during a half switching period, while continuous modes are characterized by the number of full resonant cycles that appear during a half switching period, according to [28]. A one-cycle operation of SRC# is (regardless of conduction mode) composed of a sequence of linear circuits (T1, T2, D1, D2, Q1, Q2 and X, see Fig. 7(h)), each corresponding to a particular switching interval. Every linear circuit is determined by switching certain switch pairs, as described in Fig. 7(a) to (g).

### A. Equations for subintervals

The time domain approach is used to investigate the behaviour of the SRC# operated with variable frequency and phase shift modulation. From the equivalent circuits, steady state equations of resonant inductor and capacitor voltage for every mode are derived by Laplace transform. Considering the half wave symmetry of tank variables, the analysis is performed for half cycle of switching period for every mode of operation. Similar to the work of [33] the circuit behaviour of the SRC# under each topological mode can be described using the following differential equations, for subintervals T1, D1, T2, D2, Q1, Q2, P1, P2 and X, where $V_t$ is the resonant tank voltage:

$$L_r \frac{di_{rs}}{dt} + V_{Cr} = V_t \quad (2)$$

$$C_r \frac{dV_c}{dt} = i_{rs} \quad (3)$$

$$V_t = \begin{cases} V_g' - V_o \text{ , for T1} \\ V_g' + V_o \text{ , for D1} \\ +V_o \text{ , for Q1} \\ -V_g' + V_o \text{ , for T2} \\ -V_g' - V_o \text{ , for D2} \\ -V_o \text{ , for Q2} \\ V_{Co}\text{, for X} \end{cases} \quad (4)$$

(5)

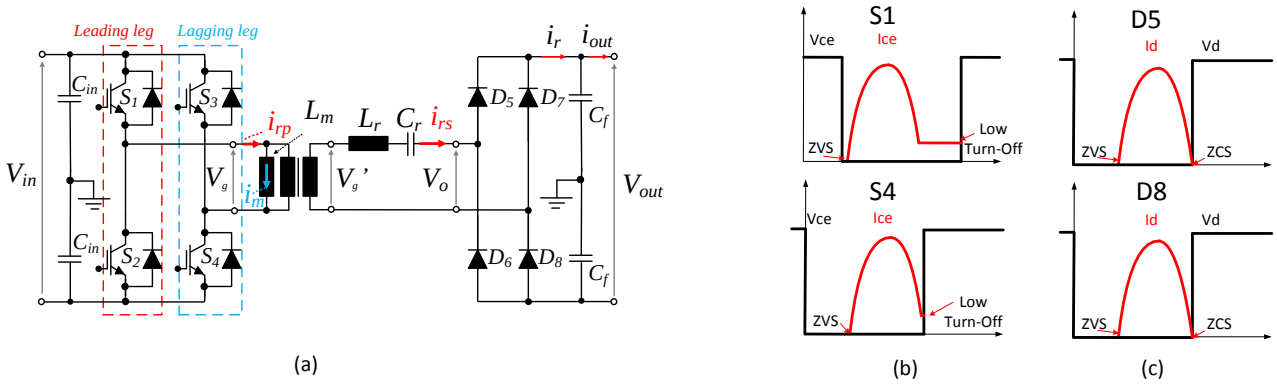


Fig. 5. SRC# (a); Switching waveforms for S1 and S4 IGBTs (b); Switching waveforms for D5 and D8 diodes (c).

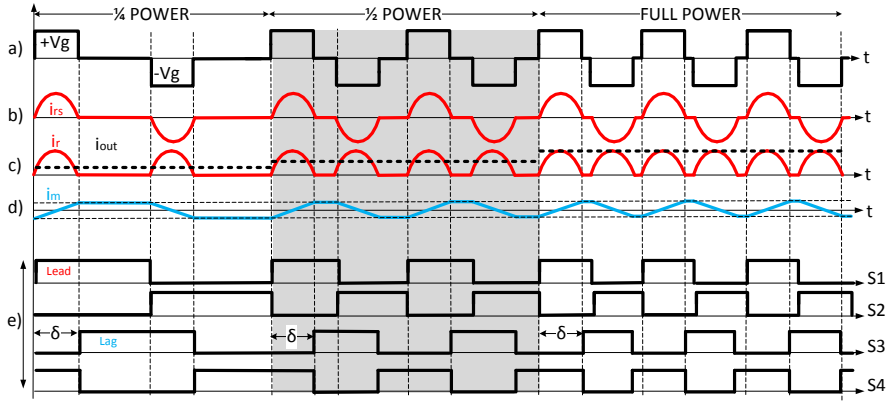


Fig. 6. Inverter output voltage $V_g$ (a); Secondary resonant current $i_{rs}$ (b); Rectifier output current $i_r$ and output averaged current $i_{out}$ (c); transformer magnetizing current $i_m$ (d); IGBTs (S1, S2, S3 and S4) switching pattern (e).

For subinterval X:

$$L_r \frac{di_{rs}}{dt} = 0 \tag{6}$$

$$C_r \frac{dV_c}{dt} = 0 \tag{7}$$

By solving these differential equations, expressions for $i_{rs}$ and $V_{Cr}$ in each subinterval can be derived, with application of the consistent initial conditions for each subinterval:

$$i_{rs} = \frac{V_t - V_{Cr}(0)}{Z_c} \sin \omega_r t + i_{rs}(0) \cos \omega_r t \tag{8}$$

$$V_{Cr} = V_t - (V_t - V_{Cr}(0)) \cos \omega_r t + i_{rs}(0) Z_c \sin \omega_r t \tag{9}$$

### B. DCM1

With reference to Fig. 8(a), $DCM1$ mode can appear in the full switching range and it's possible only if $\Delta V \approx 0$. Fig. 8(a) shows on top the applied inverter voltage $V_g'$, rectifier voltage $V_o$ and secondary resonant current $i_{rs}$. Middle graph describes resonant capacitor voltage $V_{Cr}$, primary resonant current $i_{rp}$ and magnetizing current $i_m$, while lower graph indicates the transistors (S1 to S4) switching pattern. During this conduction mode, only one half resonant cycle appears during a half switching period. This is the ideal situation for SRC#, as the power to frequency function is linear. This mode is composed of following subintervals: T1-X-T2-X. For example, during T1 subinterval [0 to $t_1$] (see Fig. 7(a)), transistors S1 and S4 are conducting and a full resonant cycle is allowed to pass. During subinterval X [$t_1$ to $t_2$], all rectifier diodes are reversed biased, as resonant capacitor voltage $V_{Cr}$ is smaller then $V_o$ and no energy can be transferred. During this subinterval, $V_{Cr}$ stays flat. Next subinterval T2 is complementary to T1, but with opposite sign.

### C. DCM2

With respect to Fig. 8(b), principle waveforms for DCM2 are shown. As the name implies two half resonant cycles will appear during a half switching period. This conduction mode can only appear in the interval [0 to $F_r/2$] and if $\Delta V > 0$. Being very similar to DCM1, DCM2 is a sequence of following sub-intervals: T1-Q1-X-T2-Q2-X, with Q1 and Q2 equivalent sub-circuits shown in Fig. 7(e) and (f). From [$t_0$ to $t_1$], S1 and S4 conduct and a full resonant cycle is delivered to the load. During this interval, as the resonant current $i_{rs}$ is increasing, resonant capacitor voltage increases too. As soon as the resonant current reaches zero, a phase displacement between S1 and S4 is applied and S1 is no longer conducting.

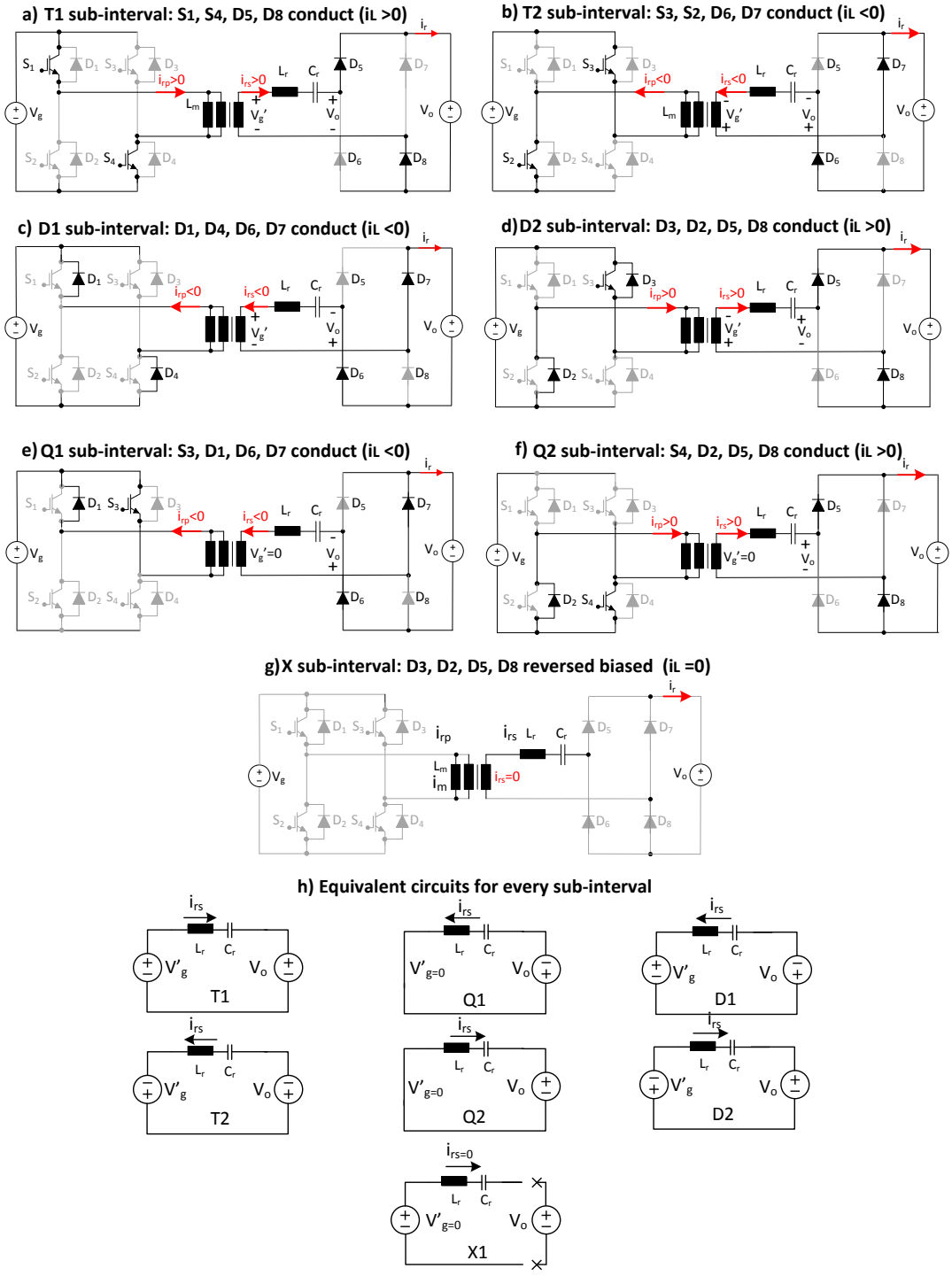


Fig. 7. T1 sub-interval (a); T2 sub-interval (b); D1 sub-interval (c); D2 sub-interval (d); Q1 sub-interval (e); Q2 sub-interval (f); X sub-interval (g); Sub-intervals equivalent circuits (h).

In the following sub interval Q1, a negative resonant current flows through D1 and T3, while $V_{Cr}$ is slowly discharged, as $V_{Cr} > V_o$. When $V_{Cr} = V_o$, another X subinterval begins and no device is conducting.

### D. CCM1-Hybrid

CCM1-hybrid mode of conduction is described in Fig. 8(c). The name *hybrid* is used as very short X sub interval (characterized by zero resonant current) will appear. First of all, this mode can appear in the switching interval [$F_{r/2}$ to $F_r$] and if $\Delta V \approx 0$. It is composed of following subintervals:T1-

This article has been accepted for publication in a future issue of this journal, but has not been fully edited. Content may change prior to final publication. Citation information: DOI 10.1109/TPEL.2017.2770220, IEEE Transactions on Power Electronics



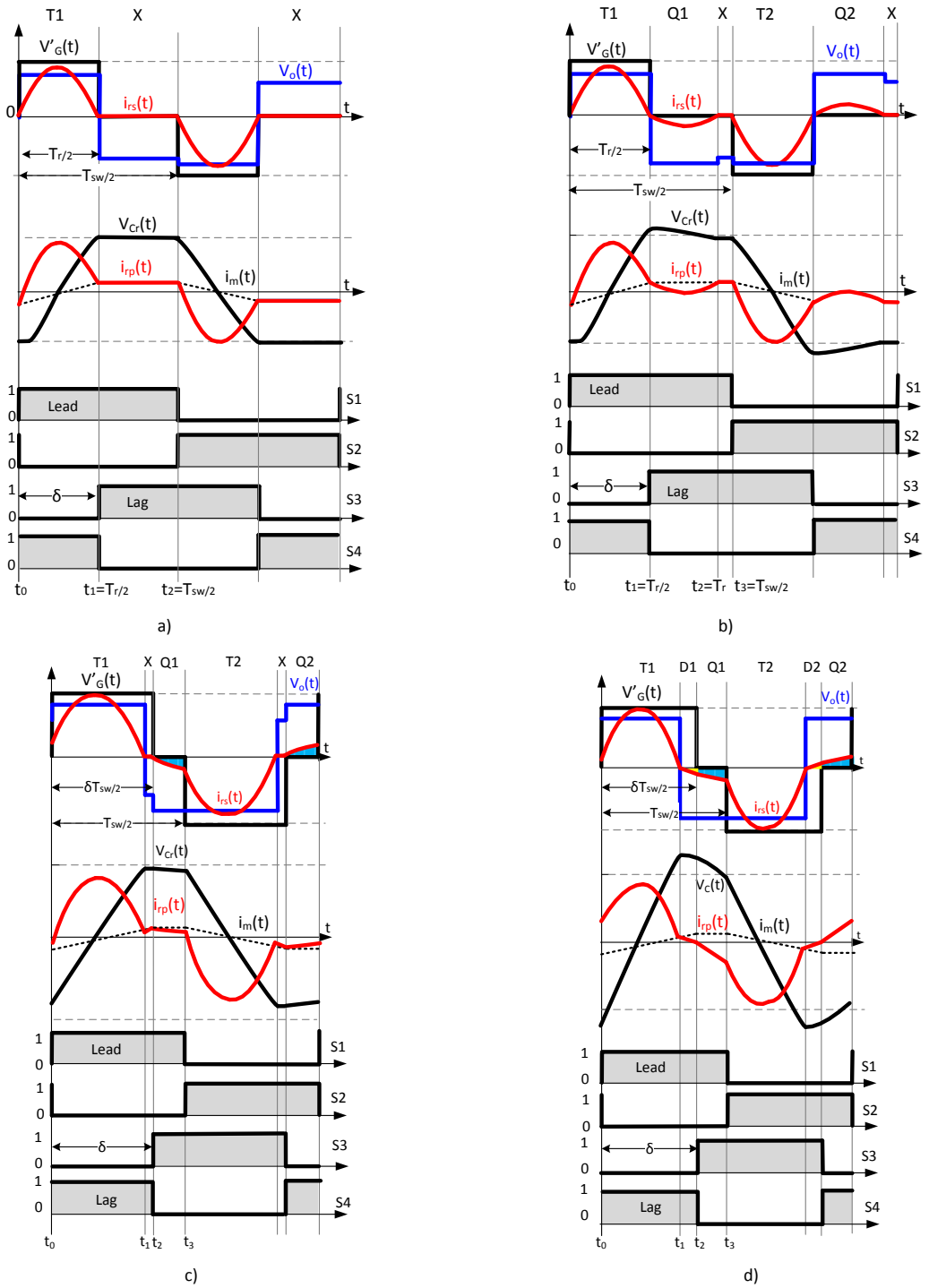


Fig. 8. DCM1 (a), DCM2 (b), CCM1-hybrid (c) and CCM1 (d) characteristic waveforms: top - inverter voltage $V_g$, rectifier voltage $V_o$, resonant secondary current $i_{rs}$; middle - resonant capacitor voltage $V_{Cr}$, primary resonant current $i_{rp}$, magnetizing current $i_m$; bottom - corresponding switching pattern.

X-Q1-T2-X-Q2. During subinterval T1, resonant current $i_{rs}$ will start at a low turn on current $i_r(0)$ and for a period equal to $\delta T_{sw/2}$ a resonant cycle is delivered to the load. Next, a X subinterval appears, as $V_{Cr} \approx V_o$. The length of T1 and X equals with $\delta T_{sw/2}$ which is the phase displacement between the inverter legs. Further on, as soon as phase displacement is implemented, a Q1 subinterval will begin and negative resonant current will start to flow. Following T2,X and Q2 subintervals are complementary, but with opposite sign. Compared to DCM1, the power to frequency relation in CCM1-hybrid is slightly non linear.

This article has been accepted for publication in a future issue of this journal, but has not been fully edited. Content may change prior to final publication. Citation information: DOI 10.1109/TPEL.2017.2770220, IEEE Transactions on Power Electronics



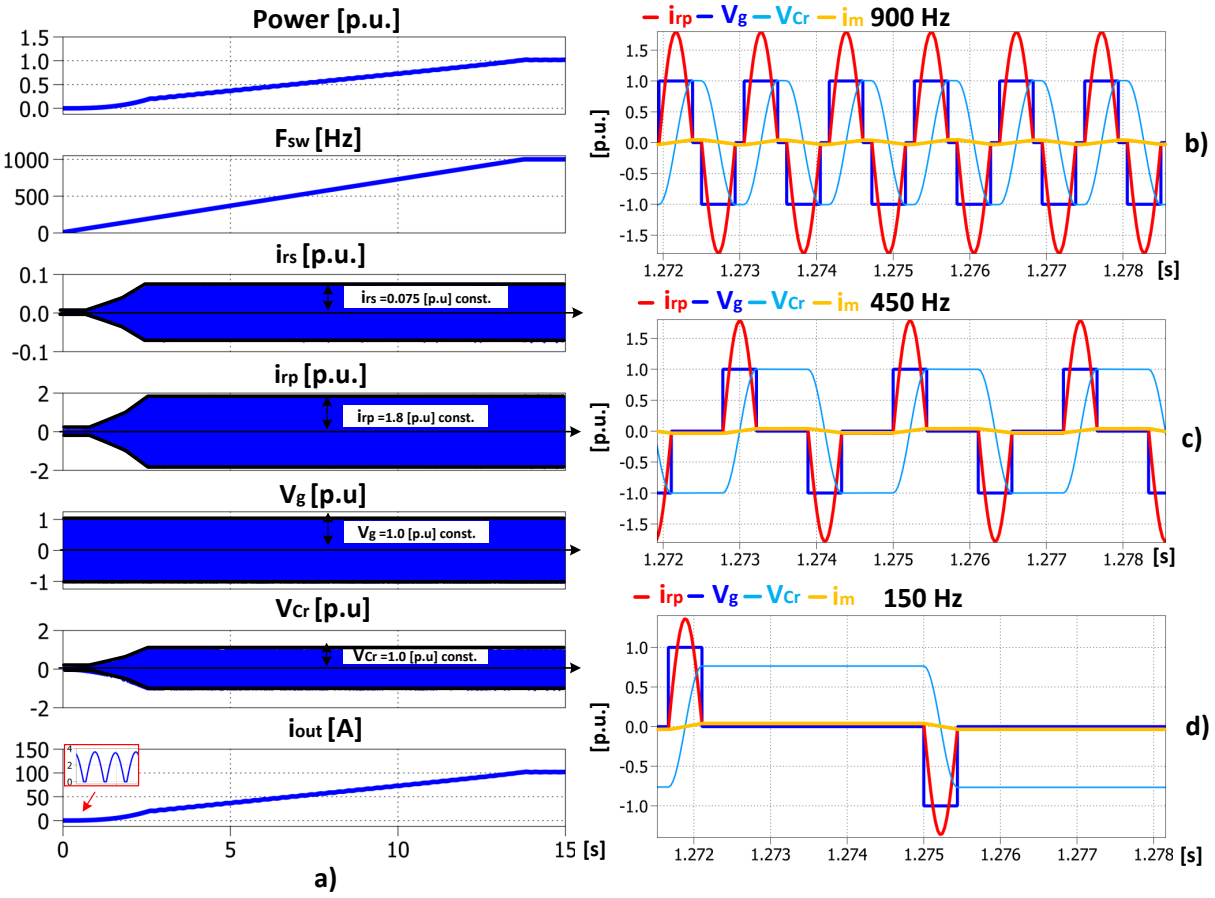


Fig. 9. Simulated results of steady state operation in DCM1 with steps in switching frequency (a); zoomed in windows of principle waveforms (primary resonant current $i_{rp}$, magnetizing current $i_m$, inverter voltage $V_g$ and resonant capacitor voltage $V_{cr}$ at 900 Hz (b), 450 Hz (c) and 150 Hz (d).

### *E. CCM1*

Final mode of conduction is characterized by the waveforms from Fig. 8(d) and it's composed of following subintervals: T1-D1-Q1-T2-D2-Q2, with equivalent circuits shown in Fig. 7. This mode appears only above $F_{r/2}$ and if $\Delta V >> 0$, showing a highly nonlinear relation between power and switching frequency and it should be avoided as it increases turn-on losses.

## IV. Steady State Operation

To illustrate the steady state operation of the target converter, a PLECS simulation model was run with different switching frequencies, in the range 0 to 1000 Hz, while voltage difference $\Delta V$ between input and output voltage was kept to 0.1%, so as to facilitate the operation in DCM1. The results are shown in Fig. 9, where it is seen that output power is linear to the applied switching frequency. As the converter operates in DCM1, peak resonant current and voltage are constant in the whole operating range. Fig. 9 (b),(c) and (d) are zoomed in windows of the principle current and voltage waveforms (primary current $i_{rp}$, secondary current $i_{rs}$, inverter voltage $V_g$, capacitor voltage $V_{Cr}$, magnetizing current $i_m$) and they also demonstrate how pulse removal technique impacts the magnetizing current, keeping it constant, regardless of applied frequency. Another aspect worthy to mention is that at very low switching frequency $F_{sw} < 50Hz$, the converter output current becomes discontinuous, as seen in Fig. 9(a-bottom). In the simulation model, LC tank quality factor $Q_s$ was considered infinite, meaning the tank has no resistive losses. In reality, to keep low losses $Q_s$ should be higher than 100, meaning very low inductor resistance and capacitor ESR. These factors are part of converter design specifications.

## V. Experiment and Discussions

In order to validate the *pulse removal technique*, control principles and protection of the SRC#, a scaled bench-top 1kW demonstrator was built with specifications as shown in Table II.

The circuit diagram is shown in Fig. 10(a) and experimental setup in Fig. 10(b). The transformer is designed for a maximum frequency of 1000 Hz, which is the same as the target component, and uses an amorphous core and windings with round wires. This demonstration was tested with operation in DCM mode, as this is the favorable mode of operation. Fig. 11 shows the SRC# characteristic waveforms for DCM1 mode, where $\Delta V \approx 0$.

This article has been accepted for publication in a future issue of this journal, but has not been fully edited. Content may change prior to final publication. Citation information: DOI 10.1109/TPEL.2017.2770220, IEEE Transactions on Power Electronics



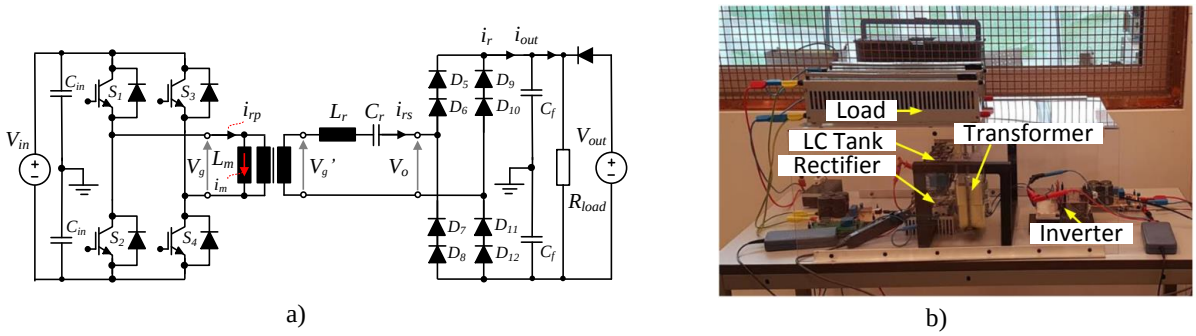


a) b)

Fig. 10. Experiment circuit diagram (a); Experiment setup (b). In order to have a constant output voltage, a second DC source is used to supply a load resistor. As long as $V_g$ is smaller then $V_o$ no power is delivered to load, as it comes only from $V_o$. If for example, the SRC# will deliver 50% of nominal load, then the external dc source will cover the rest of 50%. In this manner it's possible to obtain a constant output voltage without too much effort. The disadvantage is that the resistors are always dissipating nominal power.

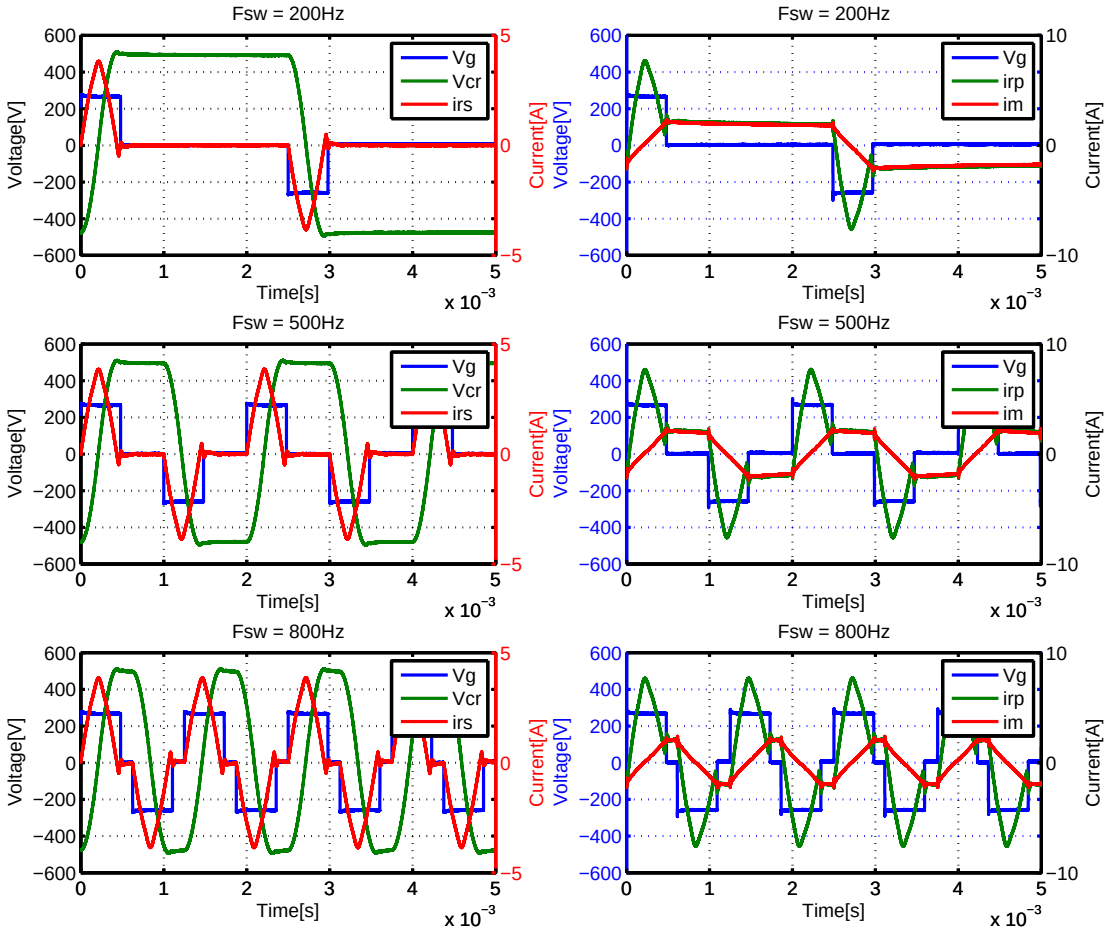


Fig. 11. Measured experimental waveforms with $\Delta V \approx 0\%$. Left side - measured secondary side resonant current $i_{rs}$, resonant capacitor voltage $V_{Cr}$ and inverter voltage $V_g$ . Right side - measured inverter side resonant current $i_{rp}$, magnetizing current $i_m$ and inverter voltage $V_g$ (b) for different switching frequencies.

Looking at principle waveforms from Fig. 11 (left side), it can be noticed that regardless of switching frequency, the magnetizing current is stable and there is no saturation phenomenon. As the transformer windings resistance is high

TABLE II
EXPERIMENTAL SRC# PARAMETERS

| Parameter | Value |
|---|---|
| $V_{in}$ | 250 V |
| $V_{out}$ | 500 V |
| $P_n$ | 1kW |
| $L_r$ | 20mH |
| $C_r$ | 2uF |
| $N$ | 2 |

in this case, as compared to the magnetizing inductance $L_m$, the magnetizing current shows a slow decline during the zero voltage period. Measurement of magnetizing current $i_m$ was possible with open transformer secondary and overlapped across $i_{rp}$ (Fig. 11 (right side).

Fig. 11 shows the primary and secondary resonant current ($i_{rp}$ and $i_{rs}$) and applied inverter voltage $V_g$ for three different switching frequencies (200, 500 and 800 Hz). It is noticed that during the zero voltage periods, on inverter side the current flowing through one pair of transistor and diodes is the magnetizing current. Another phenomenon observed during the experiments, is the acoustic noise generated, as the converter operates from very low frequency up to 1000 Hz. For elevated power, it is expected the noise to increase and it will require a system to damp the noise.

## VI. CONCLUSION

The single phase series resonant converter with resonant tank on rectifier side and operated with a new modulation scheme is proposed as a candidate for megawatt high-voltage DC wind turbines. The circuit promises high efficiency and low transformer size, due to soft-commutation on inverter and rectifier devices. This paper has given a general presentation of circuit operation, conduction modes, governing equations and sample waveforms. By employing frequency control and phase-shifted modulation below resonant point of LC tank, continuous regulation of power from nominal level to zero is possible. The main principle of proposed method is to clamp the applied voltage to zero as soon as the resonant current becomes zero, limiting the magnetic flux build-up and resulting in a compact and efficient transformer. The circuit will experience four different conductions modes (2 discontinuous and 2 continuous) and they are determined by operating frequency and voltage drop across LC tank. The proposed pulse-removal modulation scheme and the expected conduction modes were implemented and tested on a 1kW, 250V/500V demonstrator. Higher power and voltage ratings are now pursued, where loss segregation and closed-loop control will be investigated experimentally, and published.

## ACKNOWLEDGMENT

The authors would like to thank the Department of Energy technology, Aalborg University, Denmark, for the financial support.

## REFERENCES

[1] C. Meyer, *Key Components for Future Offshore DC Grids*. Ph.D. dissertation, Inst.Pow.Electr.Driv., RWTH Aachen University, 2007.

[2] A. Prasai, J. S. Yim, D. Divan, A. Bendre and S. K. Sul *A new architecture for offshore wind farms*. IEEE Trans. Power Electron., vol.23, no.3, pp. 1198-1204, May 2008

[3] M. S. Carmeli, F. Castelli-Dezza, G. Marchegiani, M. Mauri and D. Rosati *Design and analysis of a medium voltage DC wind farm with a transformer-less wind turbine generator*. Proc. 19th Int. Conf. Elect. Mach (ICEM), Sep. 2010, pp.1-6.

[4] C. Meyer and Rik W. De Doncker *Design of three phase series resonant converter for offshore DC Grids*. IEEE Ind. Appl. Ann. Meet., 2007., pp.216-223.

[5] L. Max, *Design and Control of A DC Grid for Offshore Wind Farms*. Ph.D. dissertation, Dept. Energ. Env., Chalmers University of Tech., 2009.

[6] F. Deng and Z. Chen, *Control of improved full-bridge three-level DC/DC converter for wind turbines in a DC grid*. IEEE Trans. Power Electron., vol. 28, no. 1, pp. 314324, Jan. 2013.

[7] R. Lenke, J. Hu, R. W. De Doncker, *Unified Steady-State Description of Phase-Shift-Controlled ZVS-Operated Series-Resonant and Non-Resonant Single-Active-Bridge Converters*. IEEE Ener. Conv. Congr. Exp. (ECCE), September 2009.

[8] R. Lenke, *A contribution to the design of isolated DC-DC converters for utility applications*. Ph.D. dissertation, Inst.Pow.Electr.Driv., RWTH Aachen University, 2012.

[9] K. Park and Z. Chen, *Analysis and design of a parallel-connected single active bridge DC-DC converter for high-power wind farm applications*. Proc. 15th Euro. Conf. Pow. Electron. Appl. (EPE), pp. 110, 2013.

[10] J. Jacobs, A. Averberg, and R. De Doncker, *A novel three phase series resonant converter for high power Applications*. Proc. (IEEE) 35th. Ann. Pow. Eletron. Spec. Conf., vol.3 , pp. 1861-1867, 2004.

[11] N. Denniston, A. M. Massoud, S. Ahmed, P. N. Enjeti *Multiple-module high-gain high-voltage dc-dc transformers for offshore wind energy systems*. IEEE Trans. Ind.Electr., vol. 58, no. 5, pp. 1877-1886.

[12] D. Jovcic, *Step-up DC-DC converter for megawatt size applications*. IET Power Electronics., vol. 2, no. 6, pp. 675685, 2009.

[13] D. Jovcic, *Bidirectional, high-power DC-transformer*. IEEE Trans.Power Deliv., vol. 25, no. 4, pp. 2164-2173, 2010.

[14] W. Chen, A. Q. Huan, C. Li, G. Wang and W. Gu *Analysis and comparison of medium voltage high power DC/DC converters for offshore wind energy systems*. IEEE Trans. Power Electron., vol. 28, no. 4, pp. 20142023, 2013.

[15] A. Parastar and J. Seok *High gain resonant switched capacitor cell based DC/DC converter for offshore wind energy systems*. IEEE Trans. Power Electron., vol. 30, no. 2, pp. 644656, 2015.

[16] D. Duji, F. Kieferndorf, and F. Canales, *Power electronic transformer technology for traction applications-An overview*. Proc. 7th. Int. Pow. Electron. Mot.Contr. (PEMC), vol. 16, no. 1, pp. 5056, 2012.

[17] M. Steiner and H. Reinold, *Medium frequency topology in railway applications*. Eur. Conf. Power Electron. Appl. EPE, 2007.

[18] H. Hoffmann and B. Piepenbreier, *Medium frequency transformer in resonant switching dc/dc-converters for railway applications*. Proc. 2011 14th Eur. Conf. Power Electron. Appl., pp. 18, 2011.

[19] L. Heinemann, *An actively cooled high power, high frequency transformer with highinsulation capability*. APEC. Seventeenth Annu. IEEE Appl. Power Electron. Conf. Expo., vol. 1, no. c, 2002.

[20] J. W. Kolar and G. I. Ortiz, *Solid State Transformer Concepts in Traction and Smart Grid Applications Schedule / Outline*. Epe-Pemc, pp. 1166, 2012.

[21] G. I. Ortiz, *High-Power DC-DC Converter Technologies for Smart Grid and Traction Applications*. Ph.D. dissertation, Inst.Pow.Electr.Driv., ETH Zurick, 2014.

[22] J. E. Huber and J. W. Kolar, *Analysis and design of fixed voltage transfer ratio DC/DC converter cells for phase-modular solid-state transformers*. IEEE Energy Convers. Congr. Expo. ECCE 2015, pp. 50215029, 2015.

[23] D. Rothmund, J. E. Huber, and J. W. Kolar, *Operating behaviour and design of the half-cycle discontinuous-conduction-mode series-resonant-converter with small DC link capacitors*. IEEE 14th Work.on Ctrl. and Mod. of Power Electronics, pp. 19, 2013.

[24] A. F. Wittulski and R. W. Erickson, *Steady-State Analysis of the Series Resonant Converter*. IEEE Trans. Aerosp. Electron. Syst., vol. AES-21, no. 6, pp. 791799, 1985.

[25] S. D. Johnson, A. F. Wittulski and R. W. Erickson, *Comparison of resonant topologies in high-voltage DC applications*. 2nd IEEE App.Power Electr.Conf, 1987

[26] M. Hergt, D. Kurthakoti and C. Schacherere, *Connecting power plants to high voltage networks*. U.S. Patent 0 149 509, May 26, 2016.

[27] C. G. Dincan and P. C. Kjaer, *DC-DC Converter and DC-DC conversion method*. Patent application, no. 70059, 2017.
[28] V. Vorperian and S. Cuk, *A complete DC analysis of the series resonant converter*. IEEE Pow. Electron. Spec. Conf., pp. 85-100, 1982.
[29] T. Li and L. Parsa, *Medium frequency soft switching DC/DC converter for HVDC transmission*. IEEE Ind.Electr.Conf. IECON, pp. 1599-1605, 2014.
[30] S. Fan, W. Ma, T. C. Lim and B. W. Williams, *Design and control of a wind energy conversion system based on a resonant dc/dc converter*. IET Renewable Power Gen., vol. 7, no. 3, pp. 265-274, 2013.
[31] J. Lam and P. K. Jain, *Single-stage three phase AC/DC step-up medium voltage resonant converter for offshore wind power systems*. Proc. IEEE Energy Convers. Congr. Expo. (ECCE), pp. 4612-4619, Sept.2014.
[32] M. T. Daniel, H. S. Krishnamoorthy, P. N. Enjeti, *A new wind turbine interface to MVDC collection grid with High frequency isolation and input current shapin*. IEEE Journal of Emerg. and Selec. Top. in Pow.Elec., vol. 3, no. 4, pp. 967-976, 2015.
[33] F. Tsai, P. Materu, F. C. Y. Lee, *Constant-frequency clamped-mode resonant converters*. IEEE Transactions on Power Electronics, vol.3, no.4, october 1988.

**Catalin Dincan** (S'17) received the B.Sc. degree in electrical engineering from the Technical University of Cluj-Napoca, Cluj-Napoca, Romania, in 2009, and the M.Sc. degree in power electronics and drives from Aalborg University, Aalborg, Denmark in 2011. After his studies he worked as a hardware engineer with Danfoss Solar Inverters until 2015, and currently he is working toward the Ph.D degree. His current research interests include the design of high power, medium voltage, resonant converters for offshore wind turbines.

**Philip Kjaer** (S'92-M'93-SM'11) received the M.Sc. degree in electrical engineering from Aalborg University, Aalborg, Denmark, in 1993, and the Ph.D. degree from the University of Glasgow, Glasgow, U.K., in 1997. From 1993 to 1998, he was a Research Assistant at the University of Glasgow, working with advanced control of switched reluctance machines and drives. From 1998 to 2003, he was with ABB Corporate Research, Vasteras, Sweden, where, as a Development Engineer, he worked on servo-motor-based high-voltage circuit breaker drives, factory testing of synchronous machines, power converters for HVDC power transmission, and multi-megawatt variable-speed drives. In 2003, he joined Vestas Wind Systems, Arhus, Denmark, where he holds the position as Chief Specialist for Electrical Power Technology. Since 2013, he has been associated part-time professor with Aalborg University. His research covers control and application of power electronic converters, and he has 100 journal and conference publications and more than 20 patents in this field. Dr. Kjaer is a Chartered Engineer in the U.K., a Member of the Institution of Electrical Engineers, U.K., member of FEANI, member of the Danish Academy of Technical Sciences, member of the Danish national committee of Cigr, and the recipient of the 2004 Richard M. Bass Outstanding Young Power Electronics Engineer Award.

**Yu-hsing Chen** was born in Kaohsiung, Taiwan, on December 12, 1979. He received the B.S. degree from Kun Shan University, Tainan, Taiwan, in 2002 and the M.S. and Ph.D. degrees from National Tsing Hua University, Hsinchu, Taiwan, in 2004 and 2010, respectively. His research interests include voltage sag ride-through technologies and converter controls.

**Stig Munk-Nielsen** (S'92-M'97) received the M.Sc. and Ph.D. degrees from Aalborg University, Aalborg, Denmark, in 1991 and 1997, respectively. He is currently Professor WSR at the Department of Energy Technology, Aalborg University. His research interests include LV and MV converters, packaging of power electronic devices, electrical monitoring apparatus for devices, failure modes and device test systems. In the last ten years, he has been involved or has managed 10 research projects, including national and European Commission projects.

**Claus Leth Bak** (M'1999, SM'2007) received the B.Sc. with honors in Electrical Power Engineering in 1992 and the M.Sc. in Electrical Power Engineering at the Department of Energy Technology (ET) at Aalborg University (AAU), Denmark in 1994. After his studies he worked as a professional engineer with Electric Power Transmission and Substations with specializations within the area of Power System Protection at the NV Net TSO. In 1999 he was employed as an Assistant Professor at ET-AAU, where he holds a Full Professor position today. He received the PhD degree in 2015 with the thesis EHV/HV underground cables in the transmission system. He has supervised/co-supervised +35 PhDs and +50 MSc theses. His main Research areas include Corona Phenomena on Overhead Lines, Power System Modeling and Transient Simulations, Underground Cable transmission, Power System Harmonics, Power System Protection and HVDC-VSC Offshore Transmission Networks. He is the author/coauthor of app. 250 publications. He is a member of Cigr JWG C4-B4.38, Cigr SC C4 and SC B5 study committees member and Danish Cigr National Committee. He received the DPSP 2014 best paper award and the PEDG 2016 best paper award. He serves as Head of the Energy Technology PhD program (+ 100 PhDs) and as Head of the Section of Electric Power Systems and High Voltage in AAU and is a member of the PhD board at the Faculty of Engineering and Science.